STARS

2017

Physical Hydrogeological Modeling of Florida's Sinkhole Hazard

Adam Perez
University of Central Florida

University of
Central
Florida

STARS
Showcase of Text, Archives, Research & Scholarship

PHYSICAL HYDROGEOLOGICAL MODELING
OF FLORIDA'S SINKHOLE HAZARD

by

ADAM LANE PEREZ
B.S. University of Central Florida, 2015

A thesis submitted in partial fulfillment of the requirements
for the degree of Master of Science
in the Department of Civil, Environmental and Construction Engineering
in the College of Engineering and Computer Science
at the University of Central Florida
Orlando, Florida

Spring Term
2017

ABSTRACT

Sinkholes are one of the major geohazards in karst terrain and pose a social, economic, and environmental risk. In Florida, sinkhole-related insurance claims between 2006 and the third quarter of 2010 amounted to $1.4 billion. Approximately 20 % of the United States is underlain by karst terrain formed from the dissolution of soluble rocks and is susceptible to a sinkhole hazard. Particularly, Texas, Florida, Tennessee, Alabama, Missouri, Kentucky, and Pennsylvania are known as sinkhole states.

The scope of this study is to develop a physical model to simulate sinkholes (referred to as a sinkhole simulator), which can assess the qualitative behavior of the hydrogeological mechanism of Florida's sinkhole formations. Two sinkhole simulators were developed, with the second simulator constructed to overcoming the limitations of the first. The first generation sinkhole simulator incorporated a falling head groundwater system and the sinkhole could only be observed once the ground surface was breached. The second generation sinkhole simulator incorporated a constant head groundwater system which accurately depicts field conditions and the sinkhole was able to be observed during all stages of formation within this model. In both simulators multiple hydrogeological conditions were created and water level transducers were installed at various locations within the soil profile to monitor variations in the groundwater table during the sinkhole process, this was done to investigate the soil-groundwater behavior.

Findings from this study include: 1) groundwater recharge is a critical sinkhole triggering factor, 2) the groundwater table cone of depression increases as the raveled zone or void travels up through the overburden due to sinkhole formation, 3) The cover-subsidence sinkhole failure mechanism is similar to the failure mechanism present in Terzaghi's trapdoor experiment and the

cover-collapse failure mechanism consists of four district components: failure planes with

erosion envelope, arch dropout failure, formation of elliptical void, and slope stability failure,

and 4) a strong qualitative relationship between soil strength and type of sinkhole formed (cover-

subsidence or cover-collapse) was observed.

***This work is dedicated to my mother and father**
Without their support, this work would have not been possible.*

ACKNOWLEDGMENTS

TABLE OF CONTENTS

LIST OF FIGURES

LIST OF TABLES

CHAPTER 1: INTRODUCTION

1.1 Problem Statement

Sinkholes are a feature of all karst terrain and are inherently a geological hazard which may create social, economic, and environmental harm. In Florida, three different sinkhole mechanisms are dominant, which are classified as dissolution, cover-subsidence, and cover-collapse, with the latter two being of concern in this study as a result of their relatively abrupt formation periods. Sinkhole formation is not strictly a stochastic phenomenon as observed by the distribution of reported occurrences throughout the state of Florida, with this distribution heavily concentrated around the central, west-central, and north-central part of the state. Researchers have compiled statistical data showing strong correlations between sinkhole occurrence and type of sinkhole mechanism given specific hydrological conditions and overburden compositions.

1.2 Research Objectives

Through the development and use of physical modeling, this study focuses on understanding the qualitative behavior of the hydrogeological mechanism of each the cover-subsidence and the cover-collapse sinkhole, and to differentiate between soil conditions which result in either type of formation. Hydrogeological parameters under investigation include: overburden composition, overburden density, hydrological system (falling head or constant head), and the effect of a confining strata within the soil profile. Groundwater table behavior during sinkhole formation is of concern and will be monitored by hydrostatic pressure transducers. Furthering the understanding of sinkhole mechanisms will allow for a more accurate stability analysis to be performed, and more efficient detection and mitigation techniques to be developed.

CHAPTER 2: EXPERIMENTAL STUDY ON SINKHOLES: SOIL–GROUNDWATER BEHAVIORS UNDER VARIED HYDROGEOLOGICAL CONDITIONS[1]

2.1   Introduction

Karst topography is formed by the geomorphic process involving dissolution of soluble carbonate bedrock, resulting in an underground network of drainage with high hydraulic conductivity. Sinkholes (or dolines) are a feature of all karst terrains [Waltham, 2005]. There are six classifications of sinkholes each with various equivalent names: collapse, caprock, buried, solution, dropout, and suffosion [Lowe, 2002]. The latter three are the most common types of sinkholes in Florida.

Property damages resulting from sinkholes can be substantial. The Florida Office of Insurance Regulation (FOIR) performed a data call in which 211 insurers participated. The participants reported sinkhole-related claims between the period of 2006 and the third quarter of 2010. The total cost resulting from sinkhole-related insurance claims in Florida was approximately 1.4×10^9. Surprisingly, two-thirds of the claims came from three of the 67 Florida counties: Hernando, Pasco, and Hillsborough [FOIR, 2010]. The completed insurance claim study was subsequently included in the Florida Senate interim report 2011-104, *Issues Relating to Sinkhole Insurance*. Figure 2-1 shows the type of sinkhole claims reported to the FOIR. Ultimately, these ground surface failures can be traced back to the underling karst bedrock that is so common in the Floridian region.

| (a) | (b) | (c) |
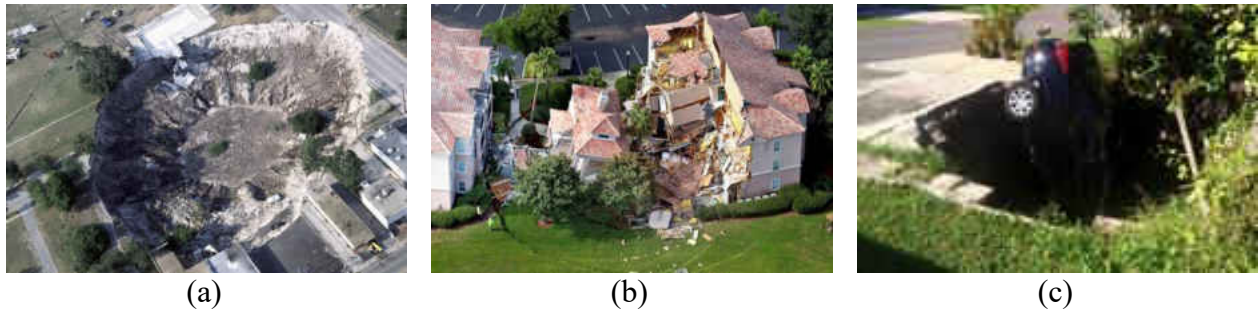
Figure 2-1. Photos of cover-collapse sinkholes in Florida: (a) Winter Park, FL (May, 1981), (b) Orlando, FL (August, 2013), and (c) Pasco County, FL (November, 2014).

Not only is there a financial risk associate with sinkholes, there is also an environmental one. Groundwaters are generally purer when compared to surface waters. The soil acts as a filter as the underlying aquifer is recharged through percolation. This process reduces the total suspended solids contained in the surface waters. When the overburden fails into the cavities formed in the bedrock, there is a direct path for surface waters to contaminate the underlying aquifer system. The 1991 lagoon collapse at the Lewiston, MN wastewater treatment facility is a relevant example of this hazard. An estimated 7.7×10^6 gal of partially treated effluent was drained into the groundwater system through a sinkhole collapse [Jannik, 1991]. The following year, there was another lagoon collapse in Bellechester, MN [Alexander, 1993]. Surprisingly, these were not the only instances in the area; two previous lagoon collapses occurred nearby in Altura, MN at the same facility during 1974 and 1976 [Liesch, 1977].

Sinkhole formation is sensitive to variations in hydraulic stresses, which may be induced by nature or human activity [Tihansky, 1999]. In a previous study by Foshee and Bixler [Foshee, 1994], there was a noticeable connection between sinkhole activity and groundwater table depression, which was monitored through the use of strategically placed piezometers around the

3

area of surface subsidence. Reinforcing this connection is the main focus of the physical soil–groundwater model testing performed in this report.

This paper presents a preliminary study on the groundwater table behavior and the effect of a clayey sand layer (impermeable layer) within the soil profile during the sinkhole process. A physical soil–groundwater model setup was developed and a series of tests were conducted under different hydrogeological conditions (e.g., with/without aquitard, partial aquitard, overburden thickness). The groundwater table at multiple locations was monitored during the sinkhole simulation process to evaluate the integrated soil-groundwater behaviors.

2.2 Background on Florida's Sinkholes

2.2.1 Sinkhole Geochemistry

Even though the geophysical relationship of the sinkhole mechanism is the main concern in this report, it is important to mention the chemistry behind the dissolution of the carbonate bedrock that ultimately sets the way for sinkhole development. Limestone ($CaCO_3$) and dolostone [$CaMg(CO_3)_2$] are the two most common carbonate sedimentary rocks. The denudation rates of these minerals depend on both chemical and mechanical weathering. Since the weathering of the carbonate rock is usually measured over geological time, the denudation rate is often expressed in the units of $m^3 \ km^{-2} \ a^{-1}$ or, equivalently, $mm \ ka^{-1}$ [Ford, 2007]. The calcite precipitation of limestone has been previously studied [Nam, 2015].

The generalized reactions involving chemical weathering of calcite and dolomite by carbonic acid are shown below. When the reverse reaction occurs, carbonates may precipitate out above cavern ceilings forming speleothems (e.g., stalactite, stalagmites, and flowstones). Kinetics of the chemical weathering is a complex process that depends on temperature, solute

4

concentration, flow rate, flow regime, surface area, pressure (for gasses), and whether there is a catalyst present. The carbon dioxide needed to form carbonic acid (H_2CO_3) is supplied by two sources, the open atmosphere and by degradation of organic matter present in the soil atmosphere. The majority of the CO_2 comes from the latter source because the open atmosphere is comprised of only 0.03 % CO_2, which lacks potential to contribute an appreciable amount of dissolved CO_2. Biogenic derived CO_2 may make up 1 %–10 % of the soil atmosphere, thus allowing for a higher potential concentration of dissolved CO_2 to occur when the water is in equilibrium [Waltham, 2005]. Ultimately, the carbonate constitutes are transported away through groundwater travel and karst features will eventually mature.

Carbonic acid:
$$CO_2(aq) + H_2O(l) \rightleftharpoons H_2CO_3(aq) \tag{1}$$

Calcite dissolution:
$$CaCO_3(s) + CO_2(aq) + H_2O(l) \rightleftharpoons Ca^{+2}(aq) + 2HCO_3^-(aq) \tag{2}$$

Dolomite dissolution:
$$CaMg(CO_3)_2(s) + 2CO_2(aq) + 2H_2O(l) \rightleftharpoons Ca^{+2}(aq) + Mg^{+2}(aq) + 4HCO_3^-(aq) \tag{3}$$
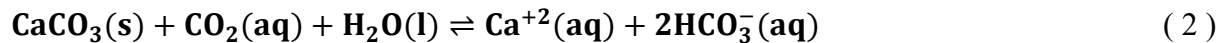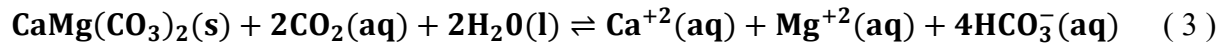
2.2.2 Sinkhole Mechanisms

The three most common types of sinkholes observed in Florida are solution (dissolution), suffosion (cover-subsidence), and dropout (cover-collapse). The mechanisms of the cover-subsidence and cover-collapse are shown in Figure 2-2. The dropout type is the most hazardous because the ground surface collapse may happen within a few hours, if not minutes. Solution sinkholes pose the least hazard because their formation happens over thousands of years, and any structure will have long expired before damages caused by surface subsidence occurs. Both the suffosion and dropout sinkholes result from the downward erosion of soils into underlying bedrock cavities. Suffosion sinkholes occur primarily in cohesionless soils; the lack of cohesive

5

forces allows the soil particles to easily migrate downward and continuously fill any void that tries to form within the overburden. A noticeable depression will develop at the ground surface because the soil is constantly raveling downward, much like an hourglass. Formation of suffosion sinkholes is on the order of months or years. Dropout sinkholes occur primarily in cohesive soils, where intermolecular forces between particles are present, allowing voids in the overburden to develop. As the void enlarges, eventually the crown of the void thins to a point at which the soils can no longer support, resulting in a collapse of the ground surface. In west-central Florida three hydrostratigraphic units are prevalent, the surficial aquifer, intermediate confining unit, and the Floridan aquifer [Copeland, 2009]. The low permeability of the confining unit allows a head differential to be possible between the surficial and Floridan aquifer system, and this in turn, increases the hydraulic load on the confining unit [Whitman, 1999].
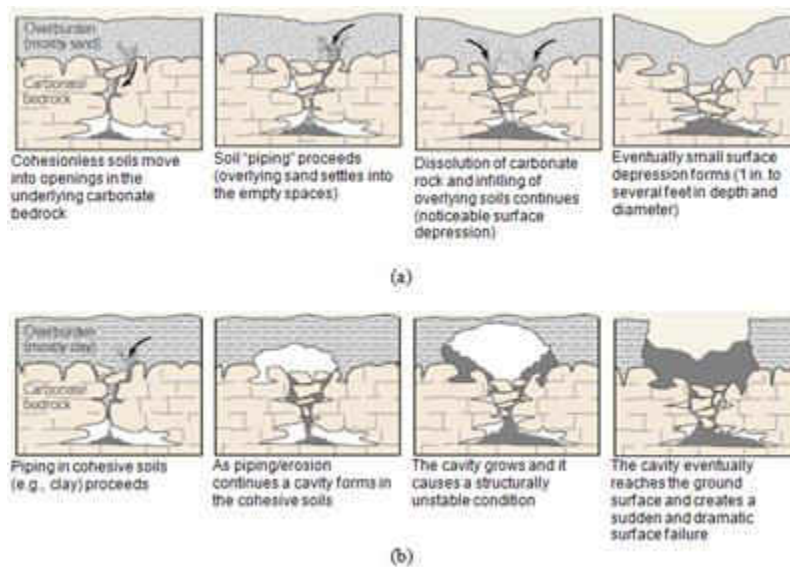
Figure 2-2. Major sinkhole types of concern in Florida: (a) cover-subsidence sinkhole, and (b) cover-collapse sinkhole [Tihansky, 1999].

2.2.3   Sinkhole Affecting Parameters

There have been multiple affecting parameters identified that contribute to the location and rate of occurrence of sinkholes. The parameters that seem to heavily influence sinkhole formation include a large head difference between the surficial and confined aquifer, recharge rate, and overburden thickness. A trend in overburden composition and type of sinkhole formed has also been observed in the field. No significant statistical relationship between surface lineament features and new sinkhole locations was found while comparing satellite imagery or low-altitude photos of linears with sinkhole occurrence data [Whitman, 1999].

While conducting their study of the Orlando area, Wilson and Beck [Wilson, 1992] observed that 85 % of new sinkholes that formed occurred within areas of high groundwater recharge. As shown in Figure 2-3, most sinkholes have been occurring in central Florida where relative high groundwater recharge exists. Whitman et al. reinforced this observation through the use of geographic information systems (GIS) software, which they used to examine the spatial interrelationships between hydrostatic heads of the surficial and confined Floridan aquifer and sinkhole occurrences in central Florida. Whitman and his team noticed a strong positive association to head differences between 5 m and 15 m and sinkhole occurrences within regions 2 km away. Heavy recharge allows a differential head to form between the surficial and confined aquifer. The higher head in the surficial aquifer induces downward seepage, which promotes erosion of the soils into the underlain bedrock cavities.

In the Orlando area, 73 % of new sinkholes occurred where overburden thickness is between 30.5 m and 48.8 m (100 ft and 160 ft) [Wilson, 1992]. A few years later, Tihansky reinforced this range of occurrence, noting that sinkholes primary occur in central Florida where

the overburden is between 9.1 m and 61.0 m (30 ft and 200 ft) [Tihansky, 1999]. In addition, it

has been noticed that sinkhole type is related to the composition of the overlying soils. An

overburden of cohesionless sands appears to form subsidence sinkholes since large cavities

cannot form because of the lack of attraction between particles. Any attempt by the soil to form a

void or arch will quickly result in a collapse; thus, the soil will continuously lose compaction and

erode downward. On the contrary, cohesive soils are able to support a void structure, because the

shear strength is also a function of cohesion and not just friction dependent on the effective

stresses confining the soil mass. The void is known to propagate upward until the crown of soil

can no longer support itself, resulting in a relatively quick ground surface failure.

Figure 2-3. Map showing reported sinkholes throughout the state of Florida.

2.3   Experimental Work

2.3.1   Testing Concept

The goal of this research is to identify and isolate the particular groundwater table

behavior that foreshadows sinkhole formation, which may be included in future methodologies

for detecting the emergence of sinkholes. The earlier the sinkhole formation is detected the

sooner soil stabilization methods can be employed to protect the ground surface against failure. To analyze the hydrogeological interaction between unconfined aquifer, aquitard, and confined aquifer, it is necessary to investigate the behaviors of different soil profiles (e.g., sand only versus sand with a clayey sand aquitard). Therefore, the setup with sand only (control setup) was performed, and this setup is shown in Figure 2-4a, which is the basis for Tests 1 and 3. Any deviation from the control's behavior could then be associated to the presence of the clayey sand layer (Figure 2-4b). Since an aquitard may be partially or fully confining, both scenarios were investigated and these are Tests 4 and 5, respectively. The opening at the bottom of the overburden causes flow of groundwater along with soil particles (referred to as soil erosion) and ultimately leads to a ground surface collapse. As the process proceeds, changes in the groundwater table (e.g., drawdown and drop) are occurring; therefore, physical features can be related to groundwater table data.
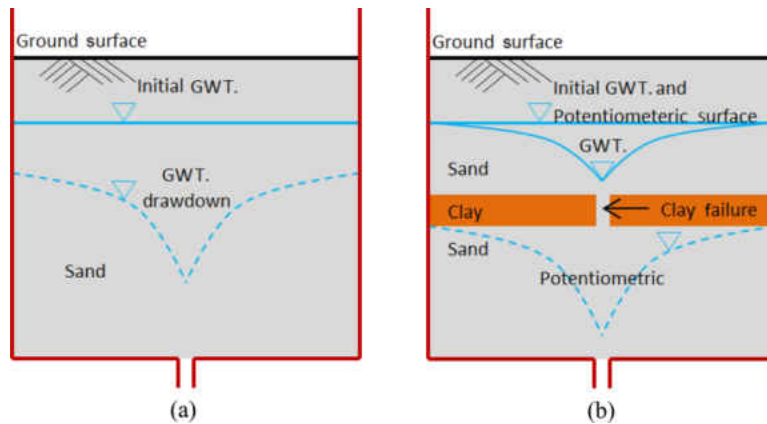
Figure 2-4. Illustration of the concepts of sinkhole testing: (a) setup with sand only, and (b) setup with sand–clayey sand–sand layers.

2.3.2   Materials

In this study, a sandy soil with 2 % passing the 200 sieve from Orlando, FL, was chosen for the physical model. The particle size distribution of the sand is shown in Figure 2-5. This soil

was classified as a dark brown, fine sand (AASHTO A-3 soil). The soil had an optimum moisture content of 13 %, a maximum dry unit weight of 16.3 kN/m^3, and a specific gravity of 2.6. The sand was compacted qualitatively in layers with a standard proctor hammer. Orange clayey sand, classified as AASHTO A-2-4 soil, was used as the aquitard. The aquitard was prepared by adding water and thoroughly mixing the clayey sand until it became a workable paste. This paste was then placed into the model with the corresponding thickness required for each trial. The surficial sand was then placed on top of the clayey sand layer. Under these conditions, the clayey sand can be considered normally consolidated. Physical soil properties are summarized in Table 2-1. The sinkhole simulator was fabricated from the bottom half of a standard 55 gal drum. It was assumed that the diameter of the drum would be large enough to observe the groundwater table drawdown without having boundary condition interference. The first step in preparing the test was to seal the opening (limestone crack) on the bottom of the metal drum using a rubber sheet. Then, an initial layer of A-3 soil with a moisture content of 13 % was well compacted in the metal drum. In this initial layer up to six PVC pipes (monitoring wells) were installed radially, with "r =" corresponding to the radial distance from the opening as seen in the figures illustrating the results. The PVC monitoring wells have an inner and outer diameter of 26 mm and 32 mm, respectively. Prior to installation, circular perforations were drilled into the wells, and then the wells were wrapped in a nonwoven geotextile. The thickness of the soil profile was varied between 10 cm and 29 cm. Individual layer thicknesses were guaranteed by chalk lines located on the inner surface of the metal drum. The surficial layer was saturated to a depth between 22.5 mm and 30 mm from the ground surface for a period of 24 h to 48 h. These water levels represent a shallow groundwater table in the soil sample.
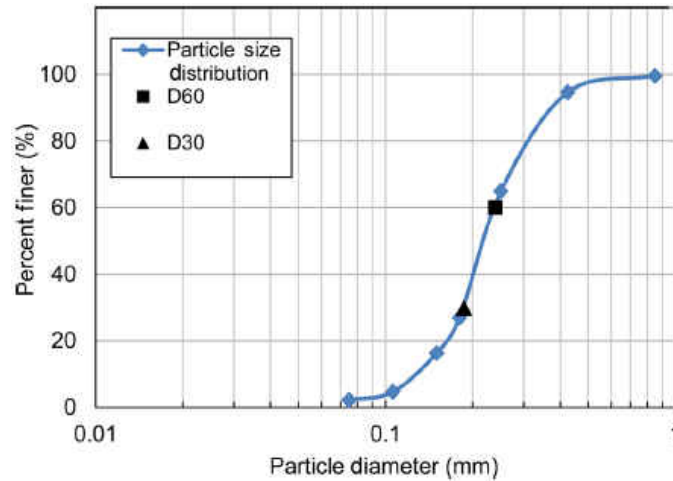
Figure 2-5. Particle size distribution of the A-3 sand used in this study.

Table 2-1. Physical soil properties of the sand and clayey sand used in this study.

Sand	A−3	Clayey Sand	A−2−4
Fines (passing 200)	2 %	Plastic limit (PL)	17 %
Uniformity coefficient, C_u	1.86	Liquid limit (LL)	23 %
Coefficient of gradation, C_c	1.13	Plasticity index (PI)	6 %
Dry unit weight, γ_d	16.3 kN/m³	Physical appearance	Orange, clayey sand
Specific gravity, G_s	2.6		
Optimum moisture content, OMC	13 %		
Physical appearance	Dark brown, fine sand		

2.3.3   Testing Setup, Sensor, and Calibration

The schematic diagram of the sinkhole physical model testing setup is shown in Figure 2-6. Soils were placed in the drum and up to six groundwater table sensors were installed. The eTape liquid level sensor (Figure 2-7a) was utilized to monitor the groundwater table drawdown. The sensor operates on a linear relationship between change in hydrostatic pressure on the sensor's envelope and change in electrical resistance. As the fluid level rises and falls, the measured resistance decreases and increases, respectively. The overall dimensions of the eTape sensor selected for the experiment are 358 mm × 25.4 mm × 0.381 mm, length, width, and thickness, respectively. The active sensing length of the sensor is 315 mm. During the

11

experiment, each sensor was in its own 26 mm inner diameter PVC monitoring well to eliminate

any lateral overburden pressure and to allow the groundwater to freely interact with the sensor.

The purpose of calibrating the sensors is to obtain linear equations, like the one seen in Figure 2-

7b, to transform the data output from resistance to water level in centimeters.
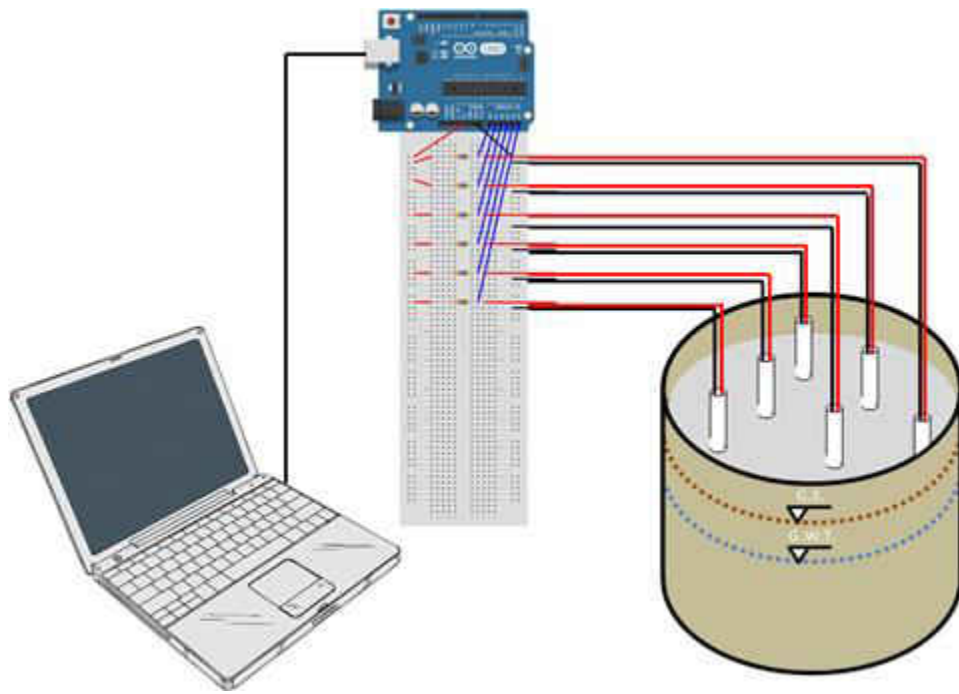
Figure 2-6. Schematic diagram of the sinkhole physical model testing setup.
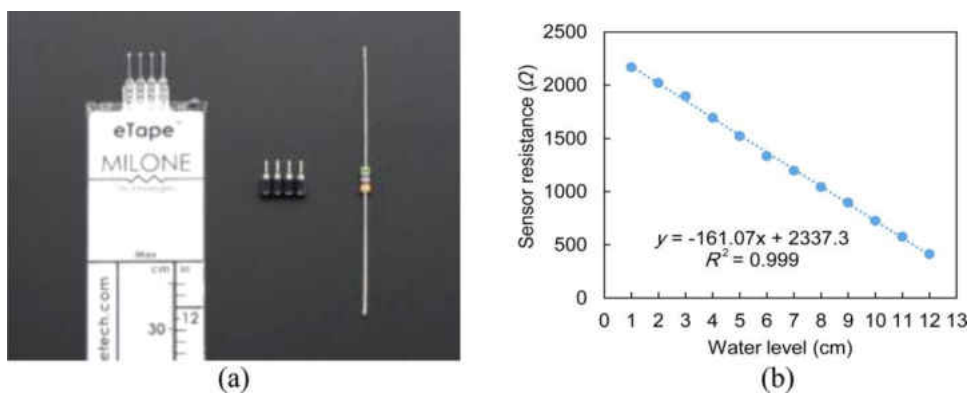
Figure 2-7. Groundwater table sensor (eTape): (a) photo of the sensor, and (b) sensor calibration curve.

To calibrate the sensors for this study a 1 L graduated cylinder, laboratory stand with clamp, breadboard with reference resistor, wired pin connector, Arduino Uno SMD, and a computer with Arduino 1.0.5 software were used. The sensor was suspended in the empty graduated cylinder by a wired pin connector joining the sensor to two wires held by clamps mounted on the laboratory stand. The two wires went to a breadboard that had a voltage divider circuit. A voltage divider circuit with a reference 560 Ω resistor was necessary to utilize the Arduino as the data logger because the analog ports of the Arduino measure voltage and not resistance. Since the reference resistor resistance was known and the voltage over the senor was being measured, the data output could be change from voltage to resistance by creating a voltage divider script and uploading the code into the Arduino unit. The linear equation was constructed by adding water, recording the corresponding resistance at each centimeter mark, and plotting the relationship.

The data acquisition system used in this study consisted of an Arduino Uno SMD, computer with Arduino 1.0.5 software, breadboard with voltage divider circuit(s), and up to six 35.8 cm long eTape liquid level sensors from MILONE Technology (PN 12110215TC-12). The Arduino module was connected to each eTape sensor by a voltage divider circuit located on the breadboard. The resolution of the eTape sensor is 0.25 mm and the sampling rate of the DAQ was 10 Hz. After the soil was saturated for a period of 24 h to 48 h and the desired groundwater level was obtained, each eTape sensor was placed into its own PVC monitoring well. The DAQ system was then turned on and started to read any water level fluctuations. After approximately 5 min of allowing the groundwater table to settle, the hole at the bottom of the drum was then opened, representing the downward erosion of the soil into the underlying bedrock cavity.

2.3.4 Testing Procedure

For sinkhole simulation testing the hole at the bottom of the drum was opened and simultaneously groundwater levels at multiple locations were continuously recorded until the surface sinkhole formed. In this study, five testing setups were prepared to evaluate the effect of varied hydrogeological conditions on sinkholes.

The experimental plan is summarized in Table 2-2. Initially, two tests were conducted to investigate the groundwater table behavior under different soil profiles: Test 1 was with sand only and one sensor and Test 2 was with layered sand–clayey sand–sand and two sensors. Test 1's setup had only a 10 cm layer of sand, while Test 2's included the sand–clayey sand–sand layers of 10–2–15 cm from bottom to top, respectively. The Test 2 setup was for simulating the aquitard separating the unconfined and confined aquifers. The inserted clayey sand layer divides the upper sand and lower sand layers. Thus, there will be no significant groundwater interaction between the unconfined and confined aquifers until collapse of the clayey sand layer. Only two groundwater table (GWT) sensors were used during this test. The GWT sensors were separately installed; for instance, one GWT sensor was placed in the lower sand layer (no perforation in the pipe extending above the clayey sand layer, thus completely blocking the intrusion of water from the upper sand layer) and the other sensor was placed right above the clayey sand layer.

Table 2-2. Experimental plan.

	Sensor Configuration	Soil Type	Soil Profile	Note
Test 1	One sensor	Sand	10 cm	Control (sand only)
Test 2	Two sensors[a]	Sand–clayey sand–sand	10–2–15 cm	For simulating the aquitard separating the unconfined and confined aquifers
Test 3	Six sensors	Sand	20 cm	Control (sand only)
Test 4	Six sensors	Sand–clayey sand–sand	10–2–10 cm	For simulating the aquitard and measuring GWT drawdown
Test 5	Six sensors[b]	Sand–clayey sand–sand	10–4–15 cm	For simulating the aquitard and measuring GWT drawdown

[a]GWT measurement at one location; one above and one below the clayey sand.
[b]GWT measurements at three locations; one above and one below the clayey sand for each location.

14

Subsequently, testing setups with six GWT sensors (at multiple locations) were carried out. Test 3 was a control setup where a 20 cm thick sand only layer was placed and saturated. Tests 4 and 5 had a clayey sand layer in the middle of the soil profile to allow its effect on the sinkhole process to be evaluated. Test 4 had the sand–clayey sand–sand layers of 10–2–10 cm from bottom to top, respectively. This setup was used to simulate the hydrogeological environment where the unconfined (surficial) aquifer and the confined aquifer have significant interaction. Water in the top and bottom sand layers were interacting through the PVC monitoring wells. All pipes were perforated along the entire depth. The aquitard did not cover the whole area (partially existed); thus, significant groundwater interaction between the unconfined and confined aquifers was possible. Test 5 had the sand–clayey sand–sand layers of 10–4–15 cm from bottom to top, respectively. In this setup, the clayey sand layer thickness was increased to 4 cm and the surficial aquifer thickness was increased to 15 cm. The clayey sand layer prevented any significant groundwater interaction between the unconfined and confined aquifers until its collapse. Six GWT sensors were installed at varying distances from the center hole, and they monitored the groundwater table drawdown during the experiment.

2.4   Results and Discussion

2.4.1   *Single GWT Measurement: Tests 1 and 2*

Test 1, which used sand only, exhibits a smooth change in the groundwater table with time (Figure 2-8a). Since the overburden was homogeneous and uniformly compacted, the groundwater flow may be considered more consistent than the sand–clayey sand–sand mixed layers. On the other hand, Test 2 shows a distinguishable transition in the groundwater table data. This transition point was most likely due to the collapse of the clayey sand layer. As stated

before, one sensor was installed in the bottom sand layer (confined aquifer) and the other sensor was installed in the top sand layer (surficial aquifer), with "top" and "bottom" corresponding to sensor locations within those aquifers, as seen in the figures illustrating the results. In Figure 2-8b, the surficial aquifer does not show a significant drop until the moment of assumed clayey sand layer collapse, which was approximately 13 min since the opening of the hole. The surface sinkhole occurred around 14 min. Figure 2-8b shows two zones: Zone 1 (before the assumed clayey sand layer collapse) and Zone 2 (between assumed clayey sand layer collapse and the surface sinkhole). The time periods of Zones 1 and 2 are about 13 min and 1 min, respectively. This indicates that the bottom soils had progressively eroded, which can be shown as the column shaped voids in Figure 2-9. When the void reached the clayey sand layer, the clayey sand structurally collapsed because of the weight of the overburden and the water in the top layer. The water level reduction rate subsequently increased in the surficial aquifer. Once the surface sinkhole occurred, a void from the bottom hole to the surface was made, resulting in a significant increase in the water level reduction rate in both the bottom and top sand layers.
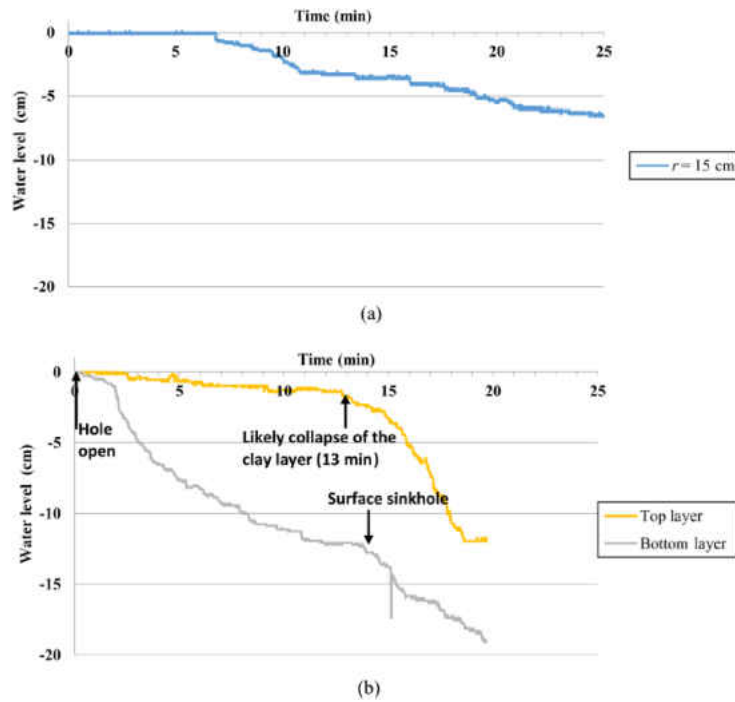
Figure 2-8. GWT data comparison of the control and sand–clayey sand–sand setups: (a) Test 1, control [sand only, radial distance (r) = 15 cm], and (b) Test 2, sand–clayey sand–sand setup.
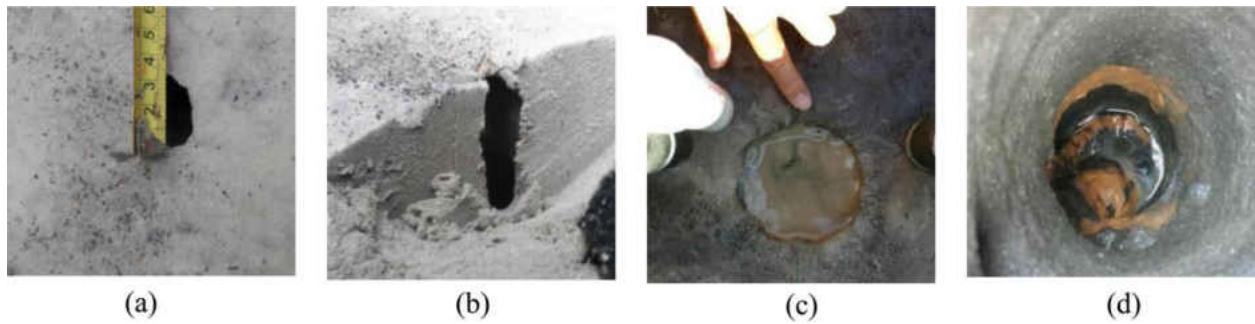
Figure 2-9. Photos of the simulated sinkhole for Tests 1 and 2 setups: (a) surface hole in Test 1, (b) longitudinal cross section of the hole in Test 1, (c) surface hole in Test 2, and (d) inside of the hole in Test 2 (note: larger size of sinkhole with clay insertion).

2.4.2   Multiple GWT Measurements: Tests 3, 4, and 5

Groundwater table sensors at multiple locations are able to illustrate the groundwater table three dimensionally, which includes the groundwater table drawdowns which change over the length of the experiment. The raw data of the groundwater table sensing for Tests 3, 4, and 5

17

are shown in Figures 2-10, 2-11, and 2-12, respectively. Each sensor continuously recorded the water level change from when the bottom hole was opened. The control setup (referred to as Test 3), shown in Figure 2-10a, shows a smooth change in the water levels along all sensors. The observation of the control setup indicates a cover-subsidence sinkhole formed, where cohesionless soil (sand) continuously moved downward as erosion continued. The groundwater table data does not show a critical transition point because the movement of sand continuously occurred. The Groundwater table cone of depression was observed by Alrowaimi et al. [Alrowaimi, 2016][Alrowaimi, 2015] (see Figure 2-10). The water level data at radial distances from the hole at each time step are plotted in Figure 2-10b, which is the time history of the groundwater table drawdown from t = 0 through t = 16 min. The sampling rate was 100 Hz (data point every 0.01 s) and a total of six groundwater table sensors were used. This cone of depression can be used to indicate the extent of erosion caused by the sinkhole process.
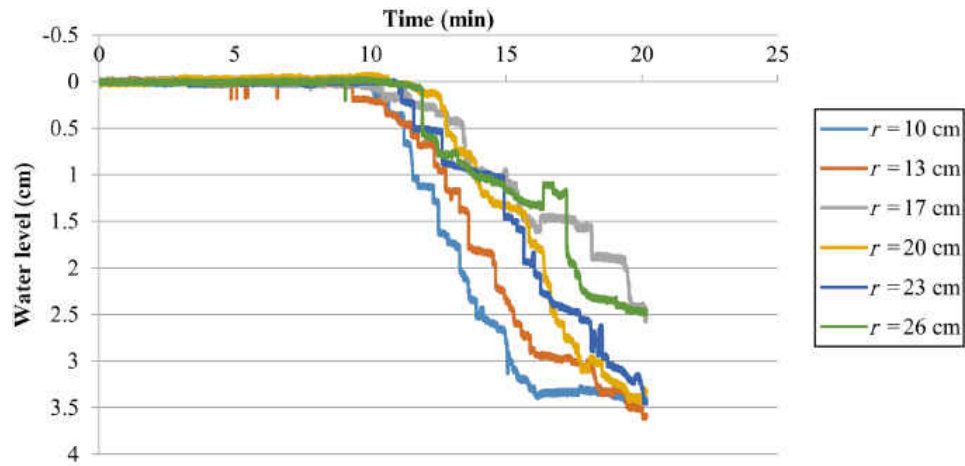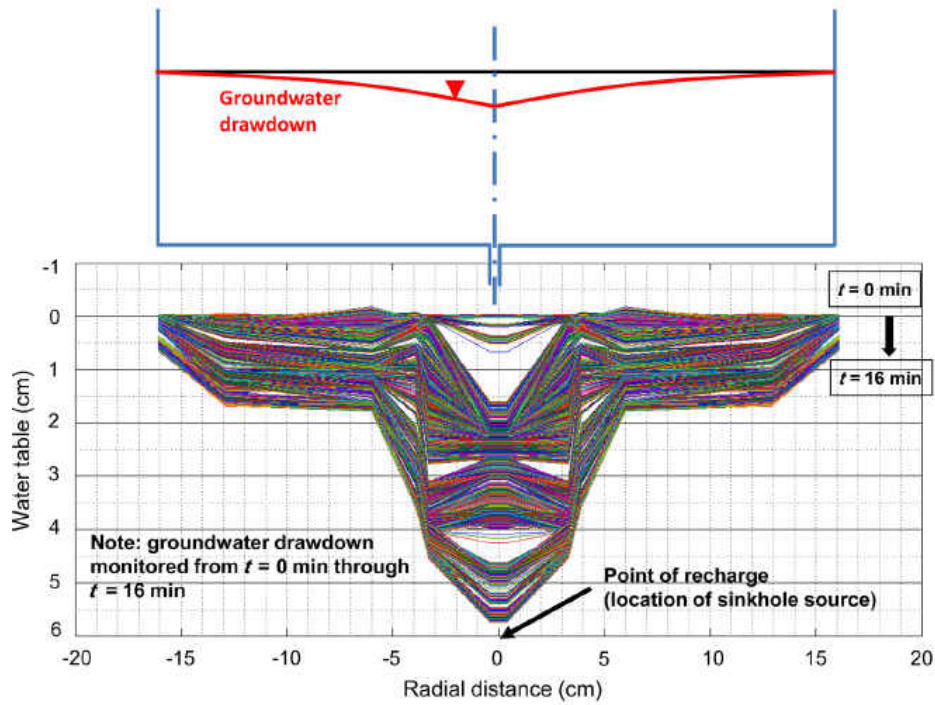
Figure 2-10. GWT data for Test 3 (control setup): (a) water level monitoring data at different spatial locations, and (b) time history of the groundwater table cone of depression measured over 16 min (with symmetric view) [Alrowaimi, 2016][Alrowaimi, 2015].
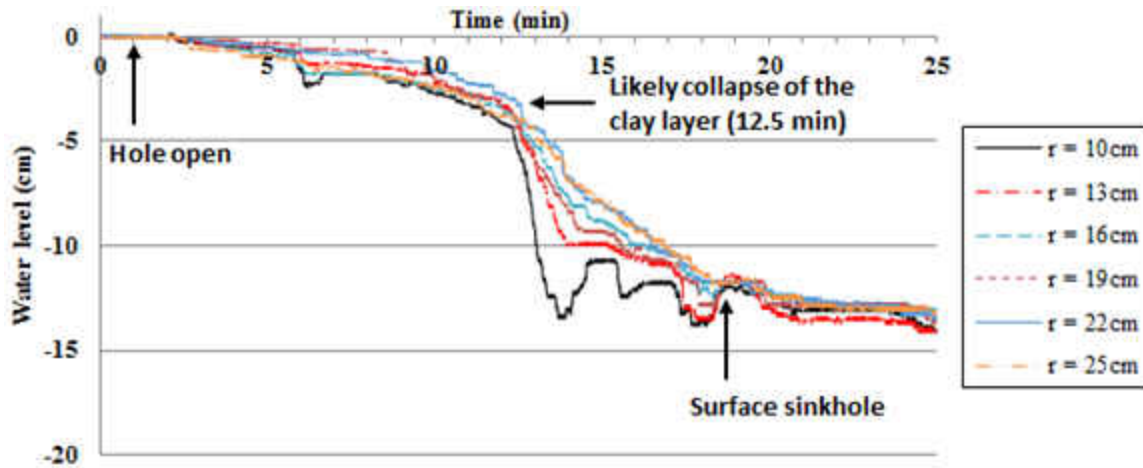
Figure 2-11. GWT data for Test 4 (partial aquitard).
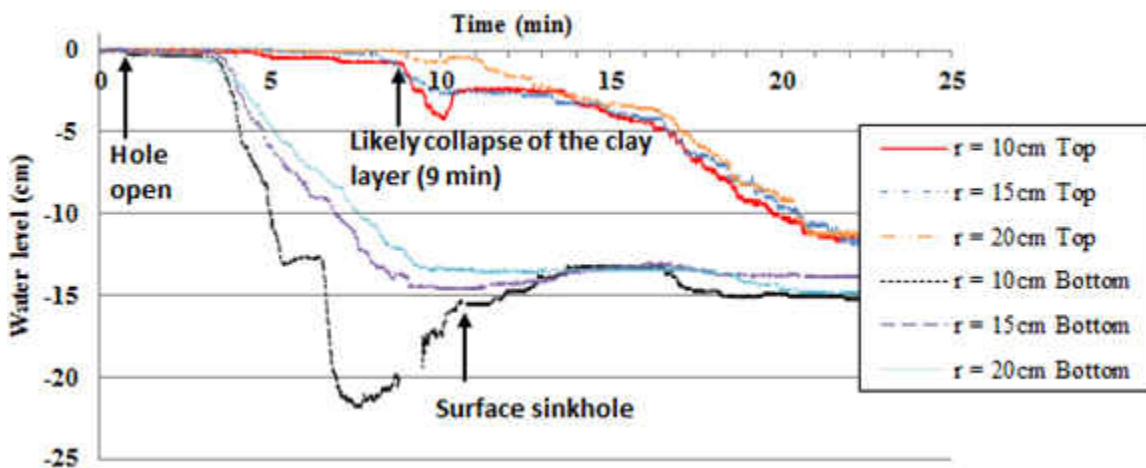
Figure 2-12. GWT data for Test 5 (complete aquitard).

On the other hand, the data of the testing setups with a clayey sand layer shows distinguishable features such as transition points and fluctuations. Figure 2-11 shows the time history of the groundwater table sensing for Test 4 where a partial aquitard (clayey sand layer) was inserted in the middle of the cohesionless overburden. Unlike Test 3 (control setup), the data shows a clear transition point at 12.5 min, as well as a water level fluctuation in sensor "r = 10 cm" (sensor closest to the hole). The transition can be explained by the collapse of the clayey sand layer; thus, the rate of the water level drop was apparently increased due to this breach. Due

to the partial aquitard (groundwater interaction between the upper and lower sands was allowed to some extent), the groundwater table was gradually lowered until the transition point (12.5 min). The groundwater table fluctuation was another phenomenon, and it can be explained by the hypothesized soil-failure mechanism which involves the sudden collapse of the soil column around the sinkhole source, unlike the continuous soil "flow" as seen in the control setups.

Test 5's setup represents the geological condition with a complete aquitard layer; the collected data is shown in Figure 2-12. Since the clayey sand layer acts as a complete aquitard, two groundwater table sensors were installed at each measurement location, one for the surficial aquifer and the other for the confined aquifer. Due to the limited number of sensors (total of six), measurements at only three locations were conducted. This setup also produces a transition point (9 min), and also a fluctuation of the groundwater table at the sensors closest to the hole. During testing, sensor "r = 10 cm bottom" (lower sand and closest sensor to the hole) exhibits substantial groundwater table fluctuation, with the lowest groundwater table level at 8 min, and loss of data between 9 to 10 min happened because of a cable disconnection. The groundwater table eventually increases in the bottom sand layer, which is probably because of recharge occurring through the breach. Unlike Test 4 (seen in Figure 2-11), no "leakage" occurs until the transition point, which can be explained by the collapse of the clayey sand layer.

2.5   Discussion

This proof-of-concept study aimed to develop an experimental setup for sinkhole simulation and to investigate the effects of different hydrogeological conditions on sinkhole formation. The physical soil–groundwater model setup can be improved by measuring and monitoring surface subsidence, mass of water and soil eroding out of the system over time, and

matric suction above the groundwater table. Above the groundwater table, the matric suction may affect the soil stability before and during the sinkhole process. The negative pore water pressure (pwp) in the partial saturated zone increases the soil stability. During the test, the surface hole first formed (with the vertical void column as shown in Figure 2-9b), and then slope failure along the sides of the hole occurred because of the reduction in negative pwp as the soil dried. In addition, significant matric suction may help to form a cover-collapse sinkhole because the negative pwp caused by capillary forces temporarily increases the stability of the soil. Therefore, as a topic of future study, it is essential to investigate the critical overburden thickness, groundwater table depth, and soil strength parameters which determine the sinkhole type, whether cover-collapse or cover-subsidence.

2.6   Conclusions and Recommendations

In this study, the groundwater table behavior in response to sinkhole formation under different hydrogeological conditions was investigated. The experimental setup included a three dimensional cylindrical physical soil–groundwater model with groundwater table sensing at multiple locations. The sinkhole was induced by opening the hole at the bottom of the physical model (simulating the bedrock cavity). Simultaneously, groundwater table changes were monitored. The experimental design included three hydrogeological conditions: (1) sand only (control setup), (2) sand–clayey sand (partial aquitard)–sand layers, and (3) sand–clayey sand (complete aquitard)–sand layers. Key findings and conclusions drawn in this preliminary sinkhole study are summarized as below:

　　　　• A sand only soil profile causes a gradual change in the groundwater table behavior

　　　　　during sinkhole formation since cohesionless soils gradually move downward as erosion

22

continues, which supports the mechanism of cover-subsidence sinkholes. On the other hand, a clayey sand layer within the overburden (aquitard) causes a distinguishable transition point in the groundwater table behavior. This groundwater table trend observed in all sensors is assumed to be related to the collapse of the clayey sand layer.

• The sensors closest to the sinkhole source show significant groundwater table fluctuation after the transition point, which is probably because of the combination of recharge from the surficial aquifer and the collapse of the "soil column" near the sinkhole source. Additionally, as the sinkhole progressed, a groundwater table cone of depression was clearly shown.

• The presence of clayey sand layers may result in larger dimensions of the surface hole. The cohesive characteristics of clayey sand can provide structural support for a short period of time, but ultimately causes more abrupt and larger surface sinks.

The hypothesis proved by this study is that the groundwater table behavior can be used to detect sinkhole formation. In addition, the behavior of the groundwater table can be a good indicator of the status of the sinkhole process. With the precursor behavior in the groundwater table, an economical in situ detection system can be developed by setting up a network of strategically placed piezometers. Groundwater table monitoring data can be used as an input to a method for sinkhole pre-detection.

CHAPTER 3: UNDERSTANDING OF FLORIDA'S SINKHOLE HAZARD: HYDROGEOLOGICAL LABORATORY STUDY[2]

3.1   Introduction

The geomorphic process involving dissolution of soluble bedrock produces what is known as karst topography. This type of terrain is associated with geologic features such as caves, springs, disappearing rivers, conical hills, and sinkholes. A network of interconnected conduits form as a result of the dissolution of soluble bedrock. When these conduits breach the rockhead the overlying soils may erode down into these highly conductive pathways, causing an extreme case of sediment transport to occur. This downward erosion, also known as "raveling", eventually leads to one of the two most common outcomes observed in Florida, a gradual subsidence of the ground surface or an abrupt collapse of the grounds surface. These two surface failures are known as either a cover-subsidence sinkhole or cover-collapse sinkhole, with the latter being the abrupt surface failure. A visual of these mechanisms is illustrated by Tihansky (see Figure 3-1). The physical properties of the overburden dictate which type of sinkhole will form. The cover-subsidence sinkhole is associated with soils with low shear resistance, such as poorly graded, loosely compacted, and/or cohesionless, whereas the cover-collapse sinkhole is associated with soils with an appreciable amount of shear resistance to allow the structural arch which crowns the void to form, such soils may have the properties of well graded, densely compacted, and/or cohesive.
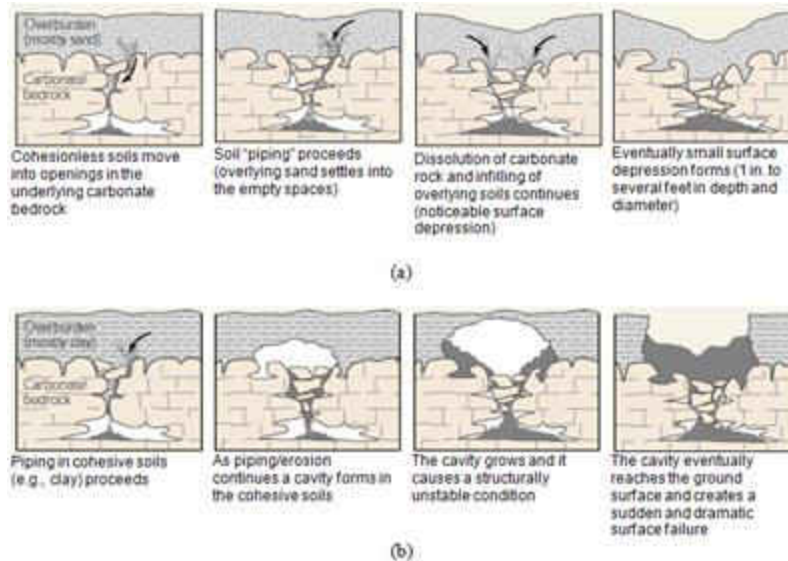
Figure 3-1. Florida sinkhole mechanisms: (a) cover-subsidence sinkhole, and (b) cover-collapse sinkhole [Tihansky, 1999].

The energy source that drives the internal erosion is the hydraulic gradient that develops due to the head difference between the unconfined and confined aquifers. Strong correlations between sinkhole development and areas of high head difference and high groundwater recharge have been observed [Wilson, 1992][Whitman, 1999][Tihansky, 1999][Xiao, 2016]. Figure 3-2 illustrates the typical hydrogeological conditions encountered in the sinkhole prone west-central Florida. Areas of recharge (downward seepage) are prone to sinkhole formation due to the development of an exit gradient, loss of stability and progressive erosion associated with the soil particles overlying the fractures in the rockhead. It has been hypothesized that in areas where the groundwater table is relatively deep and only a surficial aquifer lays above the bedrock, infiltration alone may cause the internal erosion process to occur.

Sinkholes pose a hazard socially, economically, and environmentally. The Florida Office of Insurance Regulation (FOIR) investigated the cost associated with sinkhole claims within the state of Florida. The value amounted to $1.4 billion dollars' worth of damages between 2006 and

the third quarter of 2010, with Hernando, Pasco, and Hillsborough counties accounting for two thirds of the total claims [FOIR, 2010]. Multiple cases of effluent ponds at wastewater treatment plants being drained into the underlying aquifer as a result of a sinkhole forming within them has raised environmental concerns [Liesch, 1977][Jannik, 1991][Alexander, 1993] . Traditionally sinkhole studies have been conducted by hydrogeologists; however, a clear geotechnical mechanism of sinkhole formation has not been explored.
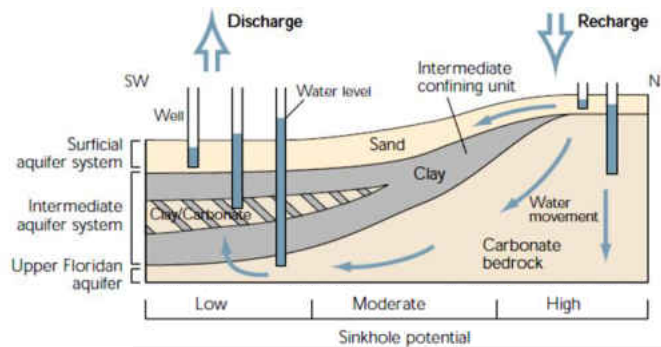
Figure 3-2. Typical hydrogeological conditions in west-central Florida [Tihansky, 1999].

This paper presents (a) the development of the sinkhole simulator, (b) the preliminary results of the sinkhole simulation tests to investigate the mechanism of two sinkhole types, and (c) a proof-of-concept test to detect and monitor the progress of a sinkhole. The sinkhole simulator incorporates a physical soil-groundwater setup under controlled hydrogeological conditions (e.g., head difference, recharge rate, flow direction, properties and thickness of overburden).

3.2   Experimental Work

3.2.1   Geomechanics-based Testing Concept

When there is a deficiency in the soil shear strength as a result of the overburden being loose and cohesionless the soil is then unable to form a large structural void and merely subsides

into the underlying cavity, much like particle flow in an hourglass. This subsiding behavior is produced by steady state displacement of the soil particles, stated differently; when the lower soil particles erode into the underlying cavity the soil particles resting upon them continuously replace them by moving downward. This steady state flow of particles produces a near instantaneous response in surface deformation as a result of the continuity of this particle replacement process. When the soil has an appreciable amount of shear strength as a result of the soil being dense with cohesion then the arching phenomenon can take place, allowing a void to form. This void is created as a result of a non-steady state flow of particles, as in more particles are leaving the system through the cavity then being replaced by particles above. Instead of a flowing action taking place throughout the whole overburden, the mode of particle transport is the result of particle detachment along the inner surface of the growing void. Eventually this void expands to the surface, leaving a structural arch of soil which is the only thing separating the ground surface from the void. When this arch becomes too thin or the void becomes too wide as a result of the particle detachment process driven by the downward seepage forces, the arch eventually reaches critical shear stress and fails. In this physical experiment the qualitative relationship of shear strength dictating the resulting type of sinkhole formation is reinforced.

3.2.2   *Materials*

Two different soils were used in this research. The first soil used was a dark brown poorly graded fine sand with 2 % passing the 200 sieve, classified as AASHTO A-3 soil, with the particle size distribution shown in Figure 3-3. Optimum moisture content of the soil was 13 %, with a specific gravity of 2.6, and a maximum dry unit weight of 104 lb/ft^3. This soil seemed

highly susceptible to liquefaction during handling. The second soil used was an orange clayey

sand, classified as AASHTO A-2-4 soil, with a plastic limit of 17 % and liquid limit of 23 %.
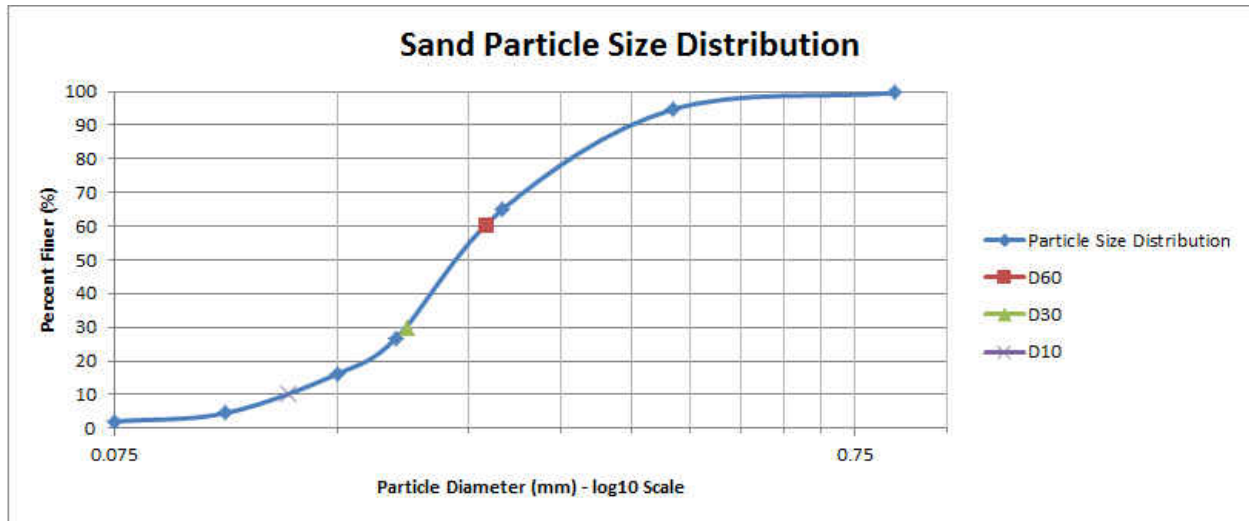
Figure 3-3. AASHTO A-3 soil particle size distribution.

3.3 Development of the Sinkhole Simulation Setup

3.3.1 Description of the Sinkhole Simulator

The physical model was constructed out of ¾" nominal size acrylic with only the soil

retaining grates varying at ¼" nominal size. The overall nominal dimensions of the model are

60" long, 40" tall, and 7.5" deep. The dimensions of the volume designated for soil placement

are 36" long, 24" tall, and 6" deep. This model incorporates unconfined and confined aquifers,

the two aquifers are connected by a ¼" wide and 5" long cut (which simulates the fracture in the

bedrock) in the internal floor that supports the soil, the cut was made lengthwise parallel to the

depth dimension. The retaining grates have a dense pattern of ¼" circular perforations and were

covered in filter paper to allow the water to infiltrate the soil in the unconfined aquifer. ¾"

valves are installed on both sides of the unconfined aquifer and one at the bottom of the confined

aquifer, as seen in Figure 3-4a. The valves are connected to a constant head system, constructed

from two 2 gallon buckets, pulleys, and ½" inner diameter flexible tubes. One bucket controls

the head in the unconfined aquifer and the other controls the head in the confined aquifer. The

constant head system is shown in Figure 3-4b.
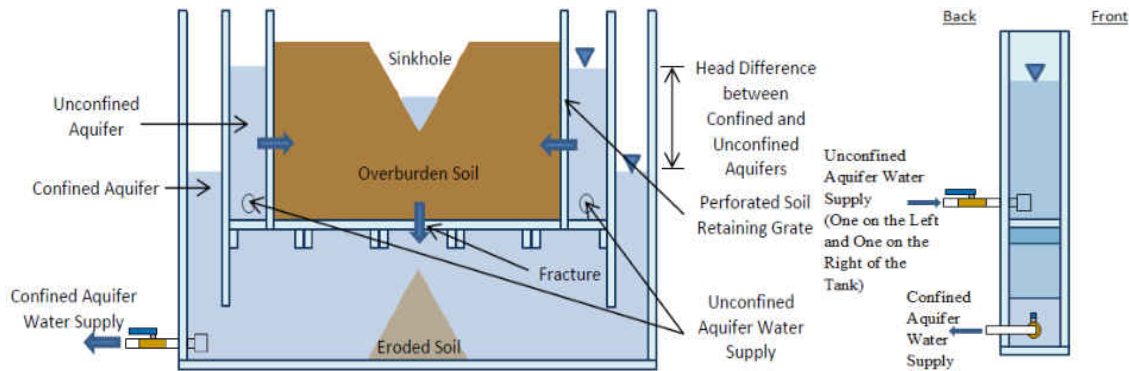
(a) Front and side view
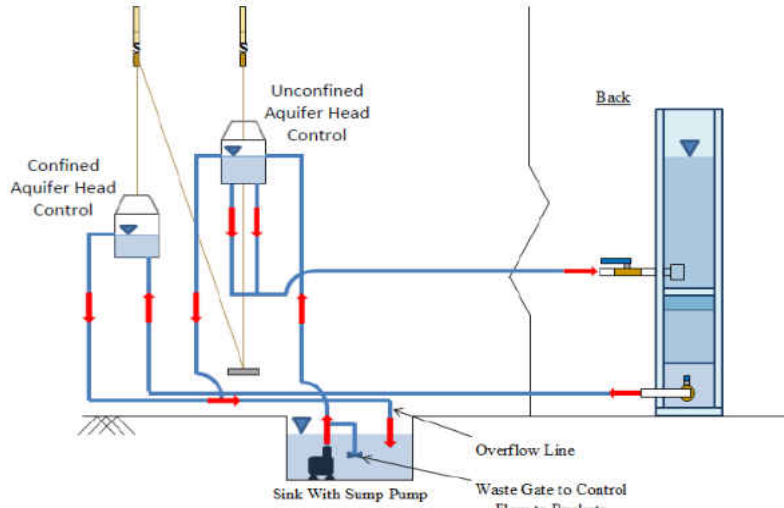
(b) Constant head system

Figure 3-4. Schematic diagrams of the sinkhole simulator (hydrogeological physical model).

3.3.2   *Groundwater Table Monitoring System*

A groundwater table monitoring system was utilized to view the groundwater table

behavior during sinkhole formation. This system was constructed from perforated PVC

monitoring wells wrapped in geotextile. The PVC pipes have a 1" inner diameter and 1.25" outer

diameter. Inside each monitoring well was an eTape liquid level sensor from MILONE

Technology (PN 12110215TC-12), Figure 3-5a and 3-5b. A change in the hydrostatic pressure

on the sensor's envelope causes a change in the electrical resistance within the sensor, this

relationship is linear. These sensors were connected to an Arduino microcontroller, which

measured the change in voltage over each sensor by the use of voltage divider circuits. Voltage

was then converted to resistance in the Arduino software. The microcontroller was connected to

a computer, which acted as the data logger.

(a)   (b)   (c)
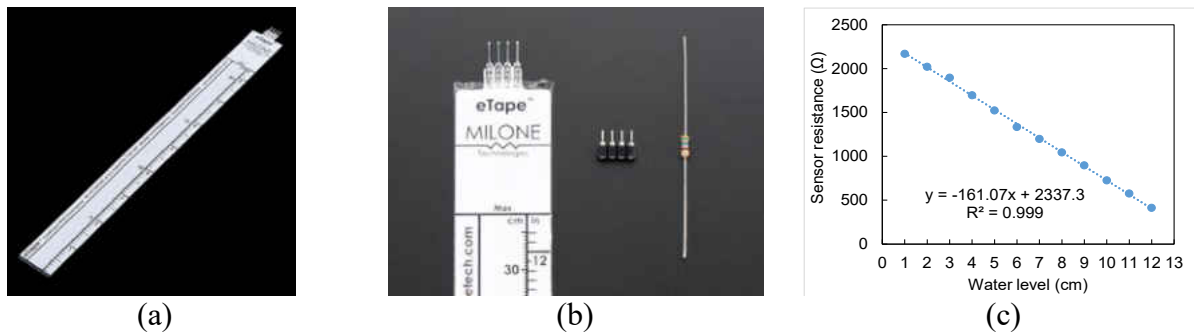
Figure 3-5. Groundwater table sensor (eTape): (a) and (b) photos of sensor, and (c) sensor
calibration curve.

3.4   Testing Procedure

This research consisted of three tests. Test #1 involved using only the A-3 soil with no

compaction effort applied to the overburden. Test #2 consisted of using a 3:1 ratio of A-3 to A-2-

4, with A-3 being the majority component; in addition compaction was applied to the soil. Test

#3 was a repeat of Test #1 but with the use of the groundwater table monitoring system. All tests

used a slightly cohesive patch placed over the fracture to prevent premature start of the

experiment when placing the soil within the model. This patch was approximately ¼" thick and

consisted of a 4:1 ratio of A-3 to clay. The experiment was initiated by causing the patch to

disintegrate by placing the aquifers in a groundwater recharge scenario.

3.4.1 Cover-subsidence Simulation (Test #1)

Test #1 used four 5 gal buckets of ground oven dried A-3 soil, which was poured into the model with no compaction effort applied. After leveling off the ground surface the overburden thickness was approximately 18". After slowly raising the water levels in both the unconfined and confined aquifers the soil was then saturated for a minimum of 48 hours. Once saturation was complete, the experiment would be initiated by lowering the water level in the confined aquifer, causing the downward seepage needed to erode the soil at the overburden-fracture interface.

3.4.2 Cover-collapse Simulation (Test #2)

Test #2 used four 5 gal buckets of ground oven dried soil with a 3:1 ratio of A-3 to A-2-4. 10 % water content by weight was added to the soil and thoroughly mixed in to aid with compaction. Each bucket of soil raised the soil profile in the physical model by approximately 6" in the loose state. After a bucket of soil was added to the model the soil was then compacted with a standard proctor hammer. A ½" thick strip of wood would be placed between the proctor hammer and the soil surface to protect the acrylic. 25 blows of the hammer would be applied to approximately 0.25 ft^2 of ground surface area. After leveling off the ground surface the overburden thickness was approximately 17". The experiment was then saturated and initiated the same way as Test #1.

3.4.3 Groundwater Table Monitoring (Test #3)

Test #3 used three 5 gal buckets of ground oven dried A-3 soil, which was poured into the model with no compaction effort applied. Unlike the previous two tests, Test #3 incorporated a groundwater table monitoring system. After approximately 6" of soil was poured into the

model, the PVC monitoring wells (casings of the groundwater table sensors) were then placed into the soil. Once the monitoring wells were in place, the rest of the soil was poured into the physical model. Four monitoring wells were placed alternating from right to left of the fracture at distances of 4", 8", 12", and 16", respectively. In addition, a control groundwater table sensor was situated in the unconfined aquifer reservoir at 20" away. The groundwater table sensors where then placed into the PVC monitoring wells and connected to the voltage divider circuits and Arduino, which in return was connected to the computer. The monitoring wells limited the overburden thickness to 12". The sensors were calibrated in situ by raising the water levels in both aquifers a few inches at a time and then measuring the resistance for that specific head of water. Five separate water level readings were used to obtain the linear equations (an equation for each sensor) which relate resistance to water level. The equations were then inserted into the Arduino water level readout script, which allowed the data to be recorded as water levels instead of resistance values. An example of the calibration plot and equation is given in Figure 3-5c. The experiment was then saturated and initiated the same way as the other two tests. The Arduino took water level readings at 10 Hz.

3.5   Results and Discussion

3.5.1   Cover-subsidence Sinkhole (Test #1)

The loose A-3 soil in combination with groundwater recharge caused a cover-subsidence sinkhole to form. Figure 3-6 shows the process of the cover-subsidence sinkhole in two stages. Before testing, the heads of the unconfined and confined aquifers are the same (Figure 3-6a), thus no soil erosion occurs (see the transparent confined aquifer). Once the experiment starts by creating confined aquifer recharge, initial surface subsidence occurs (Figure 3-6b), designated as

32

Stage 1. Continuation of the experiment causes the partially saturated soil to shear from excessive displacement (Figure 3-6c), designated as Stage 2. By the time significant surface displacement is reached it is obvious the groundwater table is below the failed surface and a drawdown is present. At the end of the experiment during draining of the unconfined aquifer the failed soil is washed out of the overburden, exposing the parabolic failure surface (Figure 3-6d).

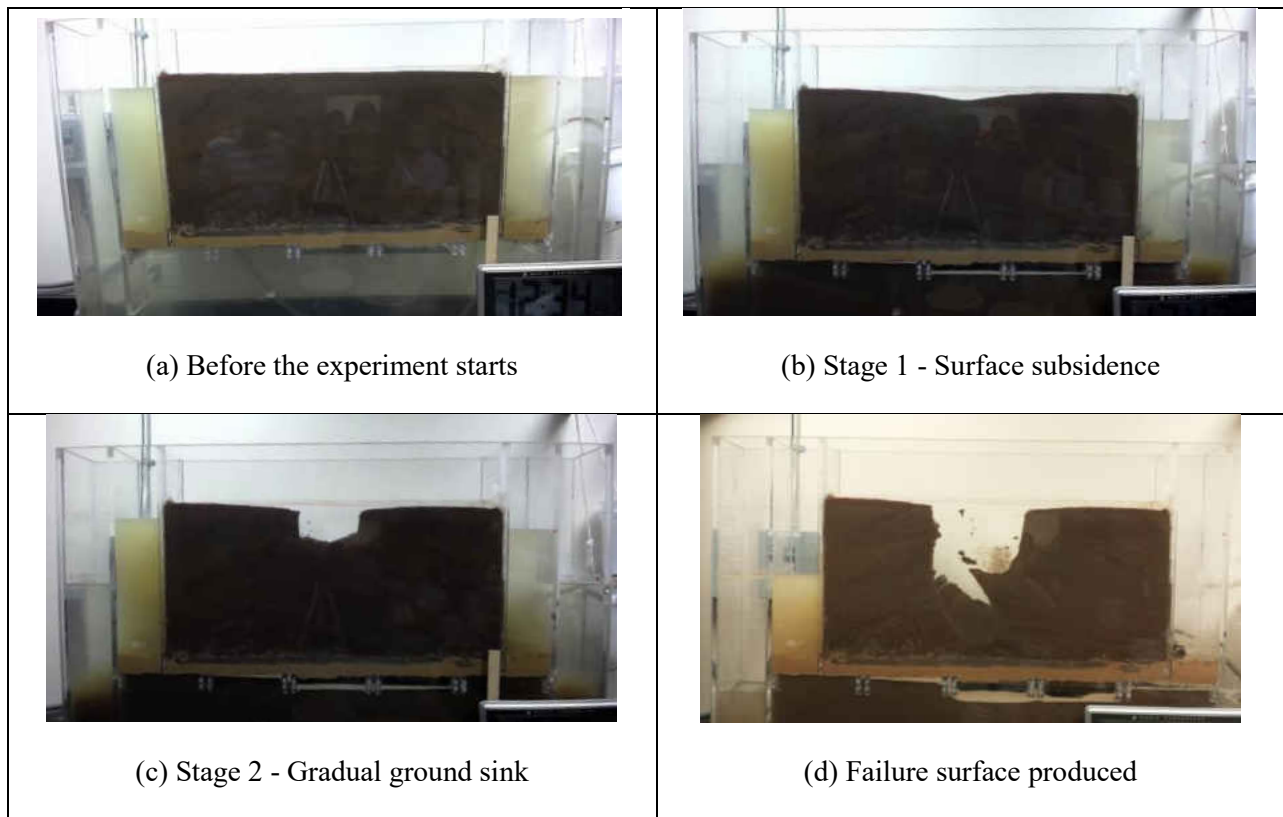|	
(a) Before the experiment starts	(b) Stage 1 - Surface subsidence
(c) Stage 2 - Gradual ground sink	(d) Failure surface produced

Figure 3-6. Test #1 images of the cover-subsidence sinkhole simulation.

The failure surface produced in the cover-subsidence sinkhole simulation (Figure 3-7a) shares a similar appearance to the failure surface produced in the trapdoor experiment (which was created using a dry cohesionless sand) (Figure 3-7b) [Terzaghi, 1943], leading to the conclusion that both of these tests share a similar failure mechanism. It is noted that the partially saturated soil allows the cover-subsidence failure surface to remain open.
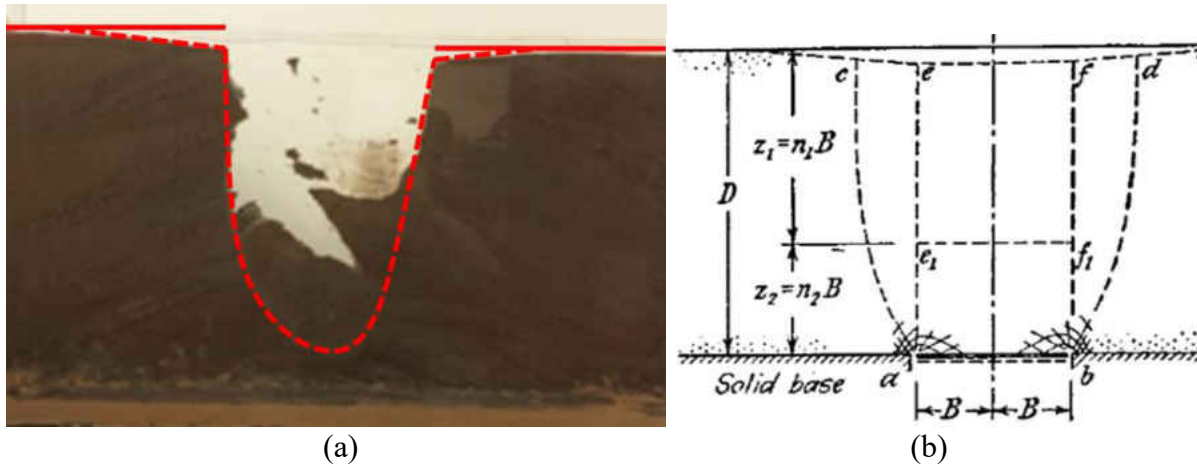
Figure 3-7. Soil failure surfaces: (a) cover-subsidence sinkhole simulation, and (b) trapdoor experiment [Terzaghi, 1943].

3.5.2   Cover-collapse Sinkhole (Test #2)

Figure 3-8 shows the evolution of a cover-collapse sinkhole from front and top views at different stages. 16 sec after opening the valve to lower the confined aquifer and with only a 1" drop in head, it was observed the soil started eroding through the fracture. 6 min into the experiment a small void was visible (Stage 1). This void would continue to grow larger by eroding soil particles from the inner surface of the void (Stage 2); however, no visible signs of surface subsidence occurred until a couple of minutes before the surface collapse, which occurred after 33 min. Eventually the void expands upward and the ground surface structurally collapses, resulting in a sinkhole (Stage 3). As the near surface soil loses stability, the 2nd failure occurs, thus the size of the sinkhole is now significant (Stage 4). It is important to note that the time of the 2nd surface failure is critical because the sinkhole growth potential after this failure would be significantly reduced due to the surrounding soil stabilizing. Stage 5 involves the increase in the groundwater table and a pond is subsequently formed, by this time the sinkhole is no longer active as a result of what appeared to be the fracture becoming clogged to some extent.
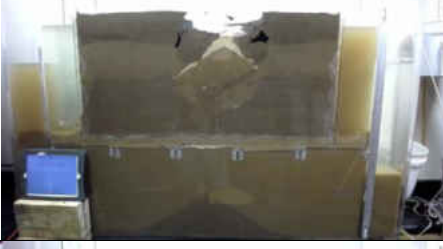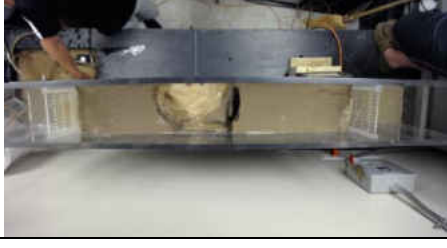
	Front view	Top view
Before the experiment starts		
Stage 1: Void initiates at the fracture interface		
Stage 2: Void expands towards the ground surface		
Stage 3: Surface collapse (with a small hole)		
Stage 4: 2nd failure with enlargement of the hole diameter		
Stage 5: The void is filled by water (making a pond)		

Figure 3-8. Test #2 images of the cover-collapse sinkhole simulation.

The cover-collapse sinkhole failure mechanism had four distinct components (Figure 3-9). During the cover-collapse sinkhole simulation it was noticed that erosion occurred above certain failure planes formed on each side of the fracture (Figure 3-9a). These failure planes occurred at angles which are likely a function of the angle of internal friction of the soil and the directional seepage forces. Both of these failure planes together create an envelope which erosion of the overburden takes place within. The more acute these angles are with respect to the bedrock, then the wider the erosion envelope, which results in a larger sinkhole. It was noticed the angles of the failure planes were unequal in the cover-collapse simulation, which might have been caused by the unequal heads in the unconfined aquifer. This unconfined aquifer head difference resulted from a combination of sediment scaling within the tubes and the unequal lengths of the tubes which connect the buckets to the unconfined aquifer, creating different total head losses to each reservoir.

The soil arch eventually drops out once the void compromises the surrounding overburden (Figure 3-9b), with the top of the arch failing in tension and the sides failing in shear, forming a small hole at the ground surface. Tension cracks appear around the periphery of the initial hole as if another arch above the failed one attempted to form, but is ultimately unsuccessful at forming since there is no soil for subsequent soil arching to take place above the ground surface. An elliptical void is formed (Figure 3-9c) and slope stability is lost at the void roof, resulting in an enlargement of the surface hole (Figure 3-9d).

(a) Failure planes with erosion envelope	(b) Arch dropout failure
(c) Formation of elliptical void	(d) Slope stability failure
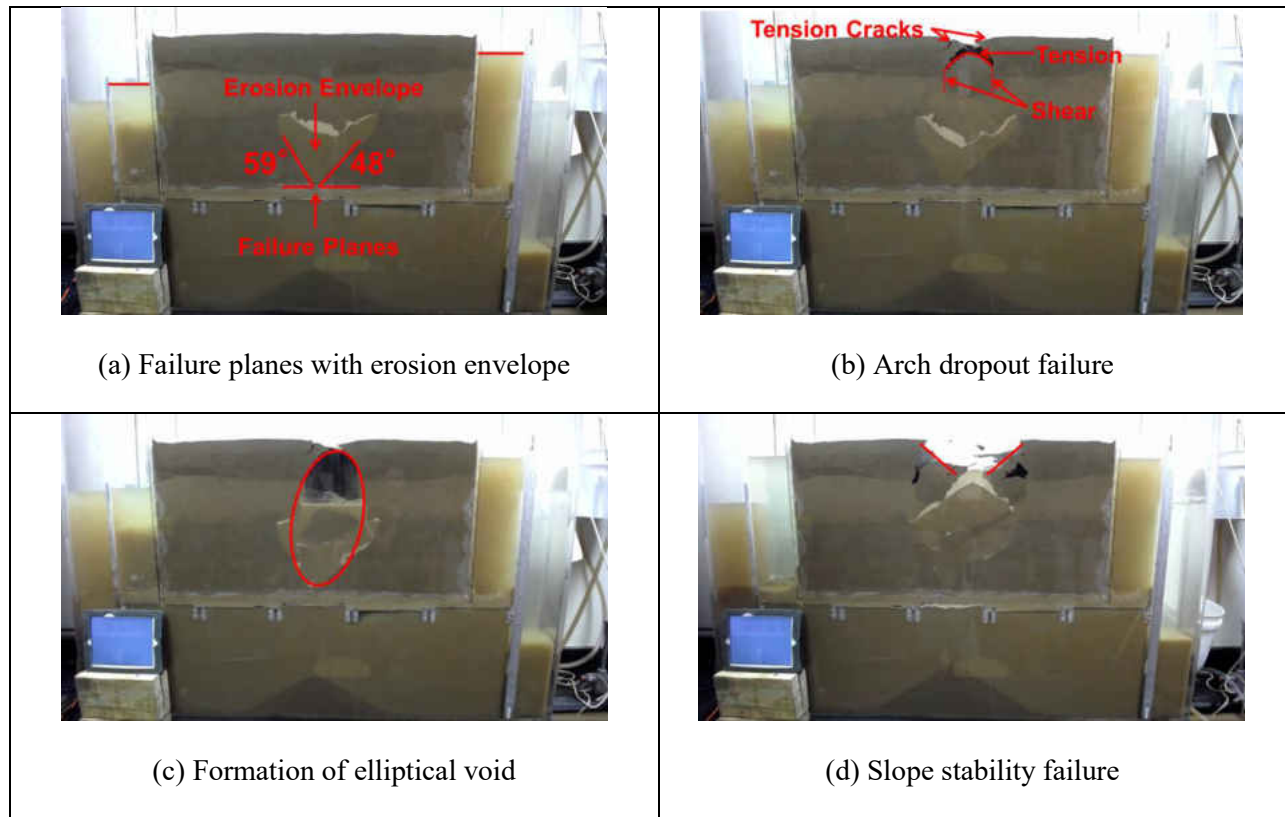
Figure 3-9. Cover-collapse sinkhole failure mechanism components.

3.5.3   *Groundwater Table Monitoring (Test #3)*

Once the head in the confined aquifer was lowered and the clayey sand patch ruptured under downward seepage, near instantaneous surface subsidence was noticed. The surface was breached by a quarter size hole within 2 min and 15 sec. A second collapse happened 5 min into the experiment. The hole continued to enlarge by eroding the perimeter. The groundwater table drawdown (Figure 3-10) leveled out after 18 min from the start of the experiment. Figure 3-10b shows the groundwater table drawdown profile with increasing distance from the fracture. The drawdown at the fracture (0") was estimated using logarithmic extrapolation (Figure 3-10b), since sinkhole groundwater table drawdown is similar to the cone of depression encountered during unconfined aquifer radial flow created by well pumping, which the logarithmic behavior

37

is expressed in the Dupuit-Thiem equation. The head difference was 6" on both sides of the

unconfined aquifer for the entire experiment. The major stages of formation are displayed in

Figure 3-11.

(a)   (b)
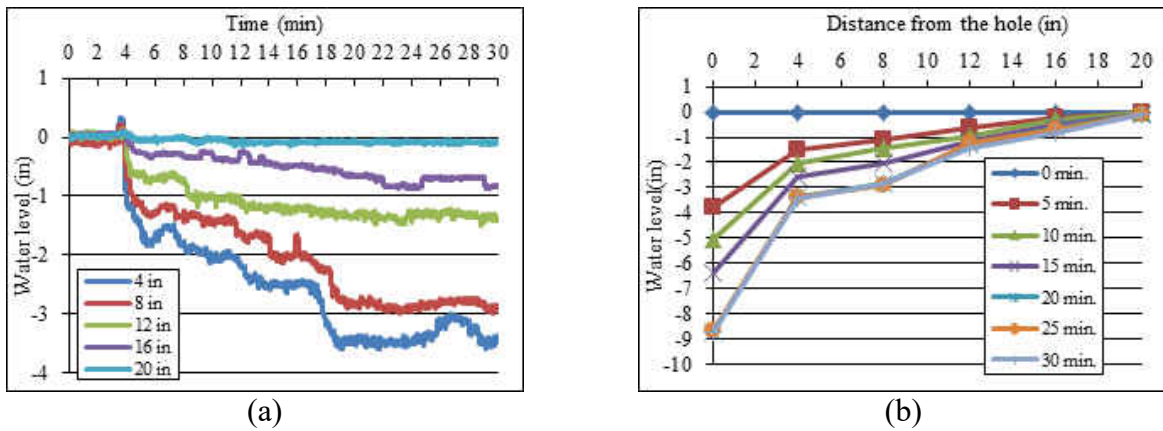
Figure 3-10. Groundwater table monitoring for Test #3: (a) groundwater table monitoring at
different linear locations, and (b) change in the groundwater table drawdown at different times.

Before the experiment starts		
Stages 1&2: Surface subsidence and gradual ground sink		
Continuous progression of ground errosion		
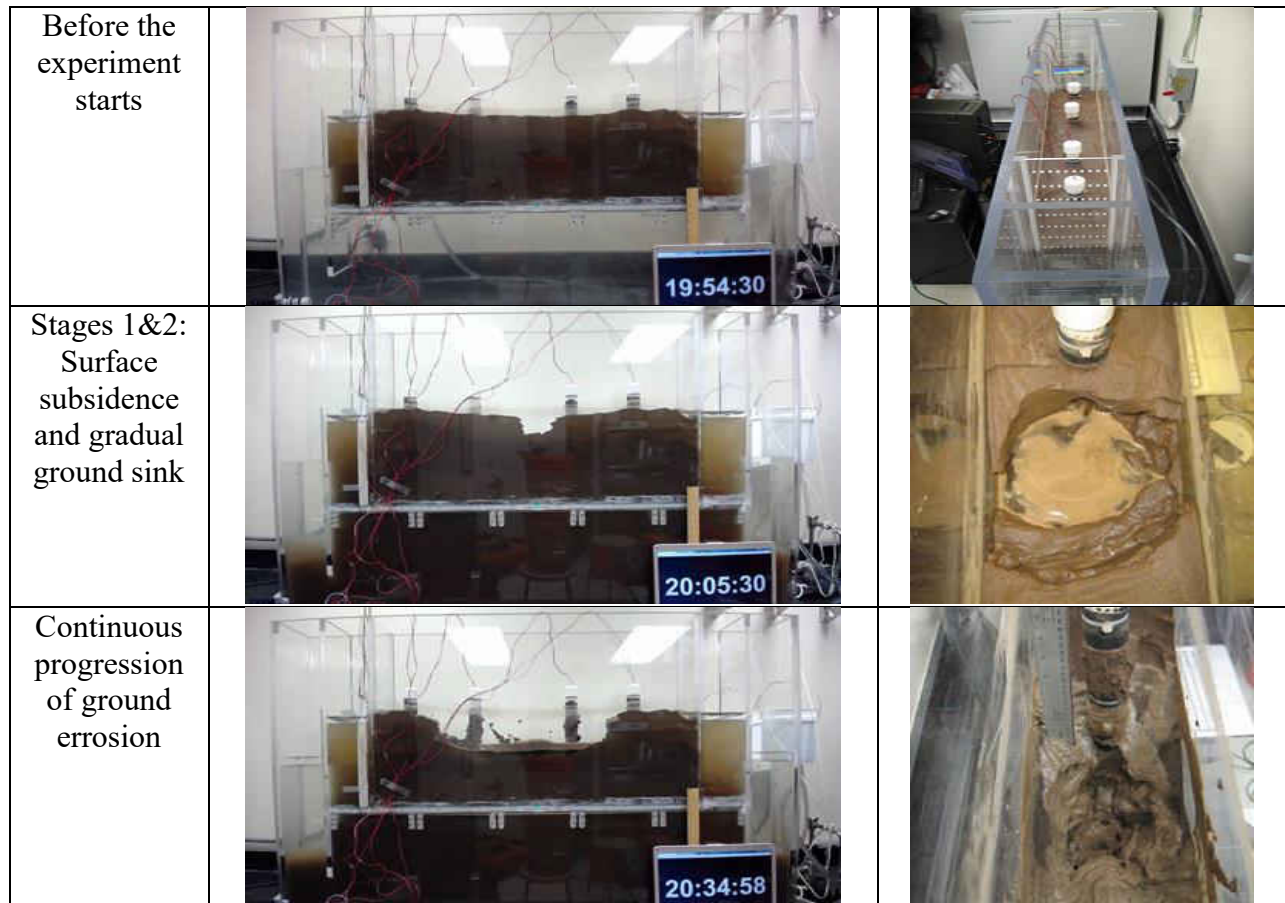
Figure 3-11. Groundwater table monitoring system during the sinkhole process (referred to as Test #3).

3.6   Conclusions

In this study, a sinkhole simulator (based on physical soil-groundwater modeling) was developed and two types of sinkholes were simulated. Although these laboratory tests form sinkholes within a short period of time, sinkhole formation typically occurs as a long-term event in the field. The groundwater behavior which is critical factor in the formation of sinkholes was monitored either qualitatively or quantitatively (Test #3) during testing. Key findings and conclusions drawn in this study are summarized as below:

• Tests #1 and #3 both simulated a cover-subsidence sinkhole, which formed due to the combination of poorly graded cohesionless sand being used and no compaction effort being applied. A near instantaneous surface subsidence progressed over time into a full surface collapse. The cover-subsidence sinkhole failure mechanism is similar to the failure mechanism present in Terzaghi's trapdoor experiment. The groundwater table drawdown continued to increase until steady state was reached, which is assumed to be a result of the flow rate between the unconfined and confined aquifers becoming constant.

• Test #2 is a good example of a cover-collapse sinkhole. A large void expanded upward and collapsed the ground surface with no initial surface subsidence observed. The cover-collapse sinkhole failure mechanism consists of four district components: 1) failure planes with erosion envelope, 2) arch dropout failure, 3) formation of elliptical void, and 4) slope stability failure. When the sinkhole is no longer active (possibly due to the fracture becoming partially clogged) the groundwater table drawdown decreases, resulting in the formation of a pond.

• As seen in Test #3, the groundwater table drawdown becomes steeper as soil raveling continues and becomes constant when erosion ceases (the sinkhole reaches equilibrium). This groundwater table drawdown monitoring concept can be applied to an in situ warning system, used to detect sinkhole development.

CHAPTER 4: CONCLUSIONS AND RECOMMENDATIONS

4.1 <u>Conclusions</u>

Finally, an overview of the major conclusions drawn from this study are summarized as below:

- Groundwater recharge is a critical sinkhole triggering factor. Recharge conditions were used to trigger sinkhole formation within the physical model and discharge conditions were used to stop premature erosion if experienced during the preparation of the experiment. Recharging of the confined aquifer occurs when the unconfined aquifer has a higher head than the confined aquifer. This downward seepage increases the effective stresses and produces an exit gradient at the overburden-bedrock fracture interface, resulting in a reduction in stability of the soil mass above the bedrock cavity.

- The groundwater table cone of depression increases as the raveled zone or void travels up through the overburden due to sinkhole formation. A conductive conduit throughout the soil profile is formed from the raveled zone or void. This conduit provides a shortened path in regards to a void, or a less restrictive path in regards to a raveled zone, for the groundwater to travel to the lower head, resulting in an increased hydraulic gradient and a steeper groundwater table cone of depression. Behavior of the groundwater table can be a good indicator of the status of the sinkhole process and monitoring of groundwater table data can be used as an input to a method for sinkhole pre-detection. It is noted that drawdown was not noticed in the unconfined aquifer until the confining layer was assumed breached, as seen in the first generation sinkhole simulator complete aquitard simulation.

- The cover-subsidence sinkhole failure mechanism is similar to the failure mechanism present in Terzaghi's trapdoor experiment. The cover-collapse failure mechanism consists of four district components: 1) failure planes with erosion envelope, 2) arch dropout failure, 3) formation of elliptical void, and 4) slope stability failure. The cover-subsidence sinkhole erosion mechanism involves a continuous flow of soil particles throughout the whole overburden resulting in a near instantaneous ground surface subsidence during formation, whereas with the cover-collapse sinkhole erosion mechanism the flow of soil particles is from the interior surface of the void and ground surface subsidence only occurs immediately before ground surface collapse.

- A strong qualitative relationship between soil strength and type of sinkhole formed (cover-subsidence or cover-collapse) was observed. Qualitatively the soil strength was increased from the cover-subsidence sinkhole simulation to the cover-collapse sinkhole simulation by the addition of a cohesive soil and by the use of compaction. In the cover-subsidence simulations the soil did not have enough strength to allow a void and structural arch to form, resulting in an erosion mechanism of a steady state flow of soil particles through the whole overburden. Once the soil strength was increased (cover-collapse simulation) the soil was able to sustain a void and structural arch, resulting in a change in the erosion mechanism to soil particle detachment along the interior surface of the void.

4.2   Recommendations

Recommendations to take into account in future studies are summarized as below:

- Investigation into the effect that directional head difference between the unconfined aquifer and confined aquifer has on the sinkhole formation rate. In all simulations the sinkholes were triggered by creating a head difference through the lowering of the head in the confined aquifer while holding the unconfined aquifer head constant, this simulated excessive well pumping of the confined aquifer, which resulted in a near instantaneous pressure change at the overburden-bedrock fracture interface. It should be investigated if this method of creating the head difference produces similar sinkhole formation rates as the alternative method, involving the increase in head within the unconfined aquifer while holding the confined aquifer head constant, simulating excessive rainfall, which would result in a delayed pressure change at the overburden-bedrock fracture interface since the pressure change would have to travel through the whole confining layer before it could influence the soil around the bedrock cavity.

- To explore the influence that head difference between the unconfined aquifer and confined aquifer has on sinkhole formation size. A study should be performed to investigate if seepage forces have a significant impact on the determination of the angles of the failure planes, thus on the erosion envelope and sinkhole formation size.

- Look into if the cover-collapse sinkhole mechanism requires cohesion. In the second generation sinkhole simulator during the cover-collapse sinkhole simulation it was noticed that during ground surface failure the top of the structural arch fails in tension, detaching from the ground surface and sliding into the void below. Under the best case

43

scenario involving a well graded, dense, and partial saturated cohesionless overburden, it is questioned if the soil has sufficient strength to allow the void and structural arch to approach the ground surface without premature failure since the soil strength would depend strictly on overburden pressure (effective stresses) and capillary forces (applicable to soil above the groundwater table), with the only resistance to tension failure being provided by the latter. If premature failure of the void happens before reaching the ground surface this could result in abrupt subsidence at the ground surface.

- Investigation into the soil in situ stress redistributions throughout the overburden caused by sinkhole formation. As the soil arching phenomenon takes place stresses are redistributed, with some zones around the sinkhole formation experiencing a stress decrease and others experiencing a stress increase. In situ pressure transducers can be used to record these stress change patterns during sinkhole formation. Behavior of the stress changes throughout the overburden can be a good indicator of the status of the sinkhole process and monitoring of stress field data can be used as an input to a method for sinkhole pre-detection.

APPENDIX: APPROVAL LETTERS

: Permission from ASTM International for using the paper entitled, 'Experimental Study on Sinkholes: Soil–Groundwater Behaviors Under Varied Hydrogeological Conditions' as the second chapter of this study.

PERMISSIONS <permissions@asce.org>

Thu 2/16/2017 3:19 PM

To:Alperez87 <Alperez87@knights.ucf.edu>;

Cc:Dickert, Donna <ddickert@asce.org>; Barbara J. Connett <bjconnett@ifai.com>;

Good afternoon Adam,

You are permitted to reuse your own in your thesis, under the condition that it does not constitutes more than 25% of your work.

A full credit line must be added to the material being reprinted. For reuse in non-ASCE publications, add the words "With permission from ASCE" to your source citation. For Intranet posting, add the following additional notice: "This material may be downloaded for personal use only. Any other use requires prior permission of the American Society of Civil Engineers."

To view ASCE Terms and Conditions for Permissions Requests:
http://ascelibrary.org/page/ascetermsandconditionsforpermissionsrequests

Authors may post a PDF of the ASCE-published version of their work on their Institutional Intranet with password protection. Please add the statement: "This material may be downloaded for personal use only. Any other use requires prior permission of the American Society of Civil Engineers. This material may be found at [URL/link of abstract in the ASCE Library or Civil Engineering Database]."

Authors may post the final draft of their work on open, unrestricted Internet sites or deposit it in an institutional repository when the draft contains a link to the bibliographic record of the published version in the ASCE Library or Civil Engineering Database. "Final draft" means the version submitted to ASCE after peer review and prior to copyediting or other ASCE production activities; it does not include the copyedited version, the page proof, or a PDF of the published version.

For more information on how an author may reuse their own material, please view:
http://ascelibrary.org/page/informationforasceauthorsreusingyourownmaterial

Hope this answers your questions.

Regards,
Leslie

Leslie Connelly
Marketing Coordinator
American Society of Civil Engineers
1801 Alexander Bell Drive
Reston, VA 20191

: Permission from ASCE for using the paper entitled, 'Understanding of Florida's Sinkhole Hazard: Hydrogeological Laboratory Study' as the third chapter of this study.

REFERENCES

Alexander, E. C., Broberg, J. S., Kehren, A. R., Graziani, M. M., and Turri, W. L., "Bellechester, Minnesota, USA, Lagoon Collapses," *Environ. Geol.*, Vol. 22, No. 4, 1993, pp. 353–361.

Alrowaimi, M., *Experimental Study of Sinkhole Failure Related to Groundwater Level Drops*, University of Central Florida, Orlando, 2016.

Alrowaimi, M., Yun, H., and Chopra, M., "Sinkhole Physical Models to Simulate and Investigate Sinkhole Collapses," *NCKRI Symposium 5: 14th Sinkhole Conference*, National Cave and Karst Research Institute, Carlsbad, NM, 2015, pp. 559–568.

Copeland, R., Upchurch, S. B., Scott, T. M., Kromhout, C., Arthur, J., Means, G., Rupert, F., and Bond, P., "Hydrogeological Units of Florida," *Special Publication No. 28 (Revised)*, Florida Geological Survey, Tallahassee, FL, 2009, pp. 1–32.

Florida Office of Insurance Regulation (FOIR), "Report on Review of the 2010 Sinkhole Data Call," 2010, http://www.floir.com/siteDocuments/Sinkholes/2010_Sinkhole_ Data_Call_Report.pdf (Last accessed 3 August 2016).

Ford, D. C. and Williams, P. F., 2007, *Karst Hydrogeology and Geomorphology*, Wiley, London, 78 pp.

Foshee, J. and Bixler, B., "Cover Subsidence Sinkhole Evaluation of State Road 434, Longwood, Florida," *J. Geotech. Eng.*, Vol. 120, No. 11, 1994, pp. 2026–2040.

Jannik, N. O., Alexander, E. C., Jr., and Landherr, L. J., "The Sinkhole Collapse of the Lewiston, Minnesota Waste Water Treatment Facility Lagoon," *Proceedings of the Third Conference on Hydrogeology, Ecology, Monitoring, and Management of Ground Water in Karst Terranes*, Maxwell House/Clarion, Nashville, TN, 1991, pp. 715–724.

Liesch, B. A., "Groundwater Investigation for the Minnesota Highway Department at the Minnehaha Park Tunnel: Minneapolis," Minn. State Project, No. 2724-78, 1977.

Lowe, D. and Waltham, T., "Dictionary of Karst and Caves," *British Cave Research Association Cave Studies Series 10*, British Cave Research Association, Buxton, UK, 2002, 40 pp.

Nam, B. H., Behring, Z., Kim, J. Y., Chopra, M., Shoucair, J., and Park, C.-S., "Evaluation of the Use of Recycled Concrete Aggregate in French Drain Systems," *J. Test. Eval.*, Vol. 43, No. 2, 2015, pp. 1–11.

Perez, A. L., Nam, B. H., Alrowaimi, M., Chopra, M., Lee, S. J., and Youn, H., "Experimental Study on Sinkholes: Soil–Groundwater Behaviors Under Varied Hydrogeological Conditions," *Journal of Testing and Evaluation*, Vol. 45, No. 1, 2017, pp. 208–219, http://dx.doi.org/10.1520/JTE20160166. ISSN 0090-3973.

Perez, A. L., Nam, B. H., Chopra, M., and Sallam, A., "Understanding of Florida's Sinkhole Hazard: Hydrogeological Laboratory Study," *Geotechnical Frontiers*, American Society of Civil Engineers, Orlando, FL, 2017.

Terzaghi, K., *Theoretical Soil Mechanics*, Wiley, London, 1943, 67 pp.

Tihansky, A. B., "Sinkholes, West-Central Florida," *Land Subsidence in the United States, Circular 1182*, D. Galloway, D. R. Jones, and S. E. Ingebritsen, Eds., U.S. Geological Survey, Reston, VA, 1999, pp. 121–140.

Waltham, T., Bell, F., and Culshaw, M., *Sinkholes and Subsidence: Karst and Cavernous Rock in Engineering and Construction*, Praxis, Chichester, UK, 2005.

Whitman, D., Gubbels, T., and Powell, L., "Spatial Interrelationships Between Lake Elevations, Water Tables, and Sinkhole Occurrence in Central Florida: A GIS Approach," *Photogram. Eng. Remote Sensing*, Vol. 65, No. 10, 1999, pp. 1169–1178.

Wilson, W. L. and Beck, B. F., "Hydrogeologic Factors Affecting New Sinkhole Development in Orlando Area, Florida," *Ground Water*, Vol. 30, No. 6, 1992, pp. 918–930.

Xiao, H., Kim, Y. J., Nam, B. H., and Wang, D., "Investigation of the Impacts of Local-Scale Hydrogeologic Conditions on Sinkhole Occurrence in East-Central Florida, USA," *Environmental Earth Sciences*, 2016, 75: 1274, doi:10.1007/s12665-016-6086-3.